A conserved function for pericentromeric satellite DNA

Madhav Jagannathan[1], Ryan Cummings[1, 3], Yukiko M. Yamashita[1, 2, 3, *]

[1]Life Sciences Institute, University of Michigan.

[2]Department of Cell and Developmental Biology, University of Michigan.

[3]Howard Hughes Medical Institute.

*Correspondence to: yukikomy@umich.edu

Abstract:

A universal and unquestioned characteristic of eukaryotic cells is that the genome is divided into multiple chromosomes and encapsulated in a single nucleus. However, the underlying mechanism to ensure such a configuration is unknown. Here we provide evidence that pericentromeric satellite DNA, which is often regarded as junk, is a critical constituent of the chromosome, allowing the packaging of all chromosomes into a single nucleus. We show that the multi AT-hook satellite DNA binding proteins, *D. melanogaster* D1 and mouse HMGA1, play an evolutionarily conserved role in bundling pericentromeric satellite DNA from heterologous chromosomes into 'chromocenters', a cytological association of pericentromeric heterochromatin. Defective chromocenter formation leads to micronuclei formation due to budding off of interphase nucleus and cell death. We propose that chromocenter and satellite DNA serves a fundamental role to achieve the universal characteristic of eukaryotic cells: full complement of the genome within a single nucleus.

Introduction

Satellite DNA is AT-rich, non-coding, repetitive DNA that is abundant in centromeric and pericentromeric heterochromatin. Unlike centromeric satellite DNA, whose function in kinetochore formation and thus chromosome segregation is well established (Willard, 1990; Sun et al., 1997; 2003), the role of pericentromeric satellite DNA remains obscure: although function for a few satellite DNA repeats has been implied in certain cellular processes such as meiotic segregation of achiasmatic chromosomes, X chromosome dosage compensation and formation of lampbrush-like loops on the Y chromosome during male meiosis (Yunis and Yasmineh, 1971; Dernburg et al., 1996; Bonaccorsi et al., 1990; Menon et al., 2014), a unifying theme for pericentromeric satellite DNA function remains elusive. Moreover, highly divergent satellite DNA sequences even among closely-related species has led to the idea that satellite DNA does not serve a conserved function and is mostly a selfish element or junk (Doolittle and Sapienza, 1980; Walker, 1971). Pericentromeric satellite DNA repeats are proposed to be sources of genomic instability, as their misexpression is associated with the formation of genotoxic R-loops and DNA damage (Zeller et al., 2016; Zhu et al., 2011; Zeller and Gasser, 2017). Most studies on pericentromeric heterochromatin have focused on the mechanisms to repress satellite DNA, and accordingly, a rationale for the very existence of pericentromeric satellite DNA is still lacking.

Cytologically, it is well documented that pericentromeric satellite DNA from multiple chromosomes is clustered into chromocenters in interphase nuclei in diverse eukaryotes including *Drosophila*, mouse and plants (Figure 1A) (Pardue and Gall, 1970; Fransz et al., 2002). While multiple factors such as epigenetic modifications and transcription of repetitive DNA from pericentromeric DNA sequences are known to be required for chromocenter formation (Probst et al., 2010; Hahn et al., 2013; Bulut-Karslioglu et al., 2012; Peters et al., 2001; Pinheiro et al., 2012), the ultimate consequences of disrupted chromocenter formation has never been addressed, leaving the function of chromocenters unknown.

In this study, we explored the role of pericentromeric satellite DNA/chromocenters by studying multi-AT-hook proteins, D1 from *Drosophila melanogaster* and HMGA1 from mouse. D1 and HMGA1 are known to bind specific pericentromeric satellite DNA, and we show that

these proteins are required for chromocenter formation. When chromocenters are disrupted in the absence of these proteins, cells exhibited a high frequency of micronuclei formation, leading to DNA breakage and cell death. We show that micronuclei are formed during interphase, by budding off the nucleus. We further show that D1 binding to target DNA sequence is sufficient to bring it to chromocenter. High-resolution imaging revealed chromatin threads positive for D1/HMGA proteins and satellite DNA that connect heterologous chromosomes. Taken together, we propose that chromocenter formation via bundling of satellite DNA from heterologous chromosomes functions as a mechanism to encapsulate the full complement of the genome into a single nucleus, and that satellite DNA is a critical constituent of the chromosome, serving an evolutionary conserved role.

Results

The multi-AT-hook proteins, *Drosophila* D1 and mouse HMGA1, bind satellite DNA and localize to chromocenters.

D1 in *Drosophila melanogaster* and HMGA1 in mouse are multi-AT-hook proteins, which are known to bind the *Drosophila* $\{AATAT\}_n$ satellite DNA (~8% of the *Drosophila* male genome) and mouse major satellite DNA (~6% of the mouse genome), respectively (Levinger and Varshavsky, 1982b; a; Rodriguez Alfageme et al., 1980; Lund et al., 1983; Goodwin et al., 1973). The $\{AATAT\}_n$ satellite is distributed across 11 loci on multiple chromosomes as visualized by DNA FISH on mitotic chromosome spreads (Figure 1B) (Jagannathan et al., 2017). However, it is typically clustered into a few foci in *Drosophila* interphase nuclei, colocalizing with D1 protein (Figure 1C). The D1/$\{AATAT\}_n$ foci stained positively for H3K9me2 in interphase nuclei (Figure 1C), a well-established characteristic of constitutive heterochromatin/chromocenters (Guenatri et al., 2004). Consistently, D1 localization on the mitotic chromosome spread showed its localization near the centromere marked by *Drosophila* CENP-A, Cid (Figure 1D). These results suggest that D1 is a chromocenter-localizing protein, via its binding to the $\{AATAT\}_n$ satellite DNA.

The mouse HMGA1 protein was originally identified as an abundant non-histone component of mammalian chromatin (Goodwin et al., 1973; Lund et al., 1983) with subsequent studies demonstrating its binding to satellite DNA (Strauss and Varshavsky, 1984; Radic et al., 1992). Mouse major satellite, which is present in pericentromeric regions of all chromosomes (Figure 1E) (Lyon and Searle, 1989), clustered into DAPI-dense chromocenters positive for HMGA1 protein (Figure 1F, Figure 1, figure supplement 1A, B), revealing an analogous relationship to D1/{AATAT}$_n$ satellite in *Drosophila*. Interestingly, we found that *Drosophila* D1 protein localizes to major satellite/chromocenters when ectopically expressed in multiple mouse cell lines (Figure 1G, Figure 1-figure supplement 1C, D), suggesting that D1 and HMGA1 may possess an orthologous and conserved function as satellite DNA/chromocenter-binding proteins.

D1 and HMGA1 are required for organizing chromocenters

We next examined the effects of *D1* mutation and siRNA-mediated knockdown of HMGA1 on chromocenters. We used two *D1* alleles, $D1^{LL03310}$ and $D1^{EY05004}$, which we show to be protein null alleles, evidenced by near-complete loss of anti-D1 antibody staining (Figure 1-figure supplement 2A-C). When these alleles were combined with the D1 deficiency allele, Df(3R)BSC666, it led to severe declustering of {AATAT}$_n$ satellite DNA (Figure 1H-J, Figure 1-figure supplement 2D-E), suggesting that D1 is required for clustering of pericentromeric satellite DNA into chromocenters. We observed D1's requirement for chromocenter formation in multiple cell types (Figure 1-figure supplement 2F-I), but we largely focused on spermatogonial cells, where the phenotypes (such as cell death) were most penetrant and severe.

We also examined the requirement for HMGA1 in mouse chromocenter formation. Following siRNA-mediated knockdown of HMGA1, which led to near complete loss of HMGA1 protein (see Figure 2D, E and Figure 2-figure supplement 1A-B, D-E for efficiencies of HMGA1 knockdown), we observed chromocenter disruption in multiple mouse cell lines (Figure 1K-M, Figure 1-figure supplement 2J-L). These results suggest that D1 and HMGA1 have an orthologous function to organize pericentromeric satellite DNA into chromocenters.

Loss of D1/HMGA1 leads to micronuclei formation.

To explore the function of chromocenters and satellite DNA, we examined the effects of *D1* mutation/HMGA1 knockdown, which showed strikingly similar phenotypes. We found that *D1* mutation as well as siRNA-mediated HMGA1 knockdown in multiple mouse cell lines resulted in a significant increase in micronuclei formation (Figure 2A-F, Figure 2-figure supplement1A-F).

Micronuclei are known to have compromised nuclear envelope integrity, leading to DNA damage and catastrophic chromosomal rearrangement therein (Crasta et al., 2012; Hatch et al., 2013). Therefore, we first examined a possible defect in nuclear envelope integrity in *D1* mutant. We found that loss of D1 led to breaching of nuclear envelope both in major and micronuclei, visualized by the cytoplasmic leakage of nuclear GFP (nlsGFP) (Figure 2G-I), suggesting that nuclear envelope integrity might be generally compromised. Consistently, we observed mislocalization of nuclear envelope proteins in *D1* mutant spermatogonia. We frequently observed that lamin often surrounded the nucleus incompletely in *D1* mutant (1.9% in control (n=52) and 68.9% in *D1* mutant (n=58)) (Figure 2J, K, arrows indicate lamin-negative regions on the nuclear membrane). We also observed cytoplasmic 'holes', which resemble the nucleus in that they exclude cytoplasmic proteins such as Vasa (Figure 2K, arrowhead), but are devoid of nuclear lamin (Figure 2K, arrowhead). These 'holes' were often surrounded by an ER marker, which normally surrounds the nuclear envelope (Figure 2J) (Dorn et al., 2011). Similarly, Otefin, an inner nuclear membrane LEM-domain protein (Barton et al., 2014), also showed perturbed localization (2.7% in control (n=109) and 24.5% in *D1* mutant (n=106)) (Figure 2L, M, arrows indicate lamin/Otefin negative regions on the nuclear envelope while the arrowhead indicates Otefin-positive micronuclei). Taken together, these results show that *D1* mutant cells exhibit compromised nuclear envelope integrity, which is associated with micronuclei formation.

Loss of D1/HMGA1 leads to accumulation of DNA damage

It has been shown that defects in nuclear envelope integrity can lead to extensive DNA damage in the major nucleus and micronuclei (Raab et al., 2016; Denais et al., 2016; Zhang et al., 2015; Crasta et al., 2012; Hatch et al., 2013). Nuclear envelope defects and extensive DNA damages there in lead to catastrophic chromosomal breaks/rearrangements termed chromothripsis (Crasta et al., 2012; Hatch et al., 2013). Such catastrophic DNA breaks/rearrangements are speculated to lead to tumorigenesis (Hatch and Hetzer, 2015).

Consistent with defective nuclear envelope integrity, we observed extensive DNA damages in both major and micronuclei (Figure 3A-F, arrows point to damaged DNA in micronuclei in B and D). Likely as a result of DNA damage and defective nuclear envelope integrity, *D1* mutant testes rapidly degenerated (Figure 3 –figure supplement 1A, B). When *Omi*, a gene required to promote germ cell death (Yacobi-Sharon et al., 2013), was knocked down in *D1* mutant testes, it restored the cellularity in *D1* mutant testis (Figure 3-figure supplement 1C-D), but the surviving cells showed a dramatic increase in DNA damage (Figure 3-figure supplement 1E-F). Under these conditions, surviving germ cells in *D1* mutant testes showed high frequency of chromosome breaks compared to control (3.7% in control (n=27) vs. 15.8% in *D1* mutant (n=57)) (Figure 3G, H, arrowheads indicate sites of chromosome breaks). These results show that loss of D1/HMGA1 results in compromised nuclear envelope integrity, leading to extensive DNA damage and chromosomal breaks.

Micronuclei formation in *D1* mutant/HMGA1 knockdown cells is due to budding from nucleus during interphase.

It has been shown that micronuclei form by lagging chromosomes (Crasta et al., 2012). Thus, we examined whether *D1* mutation/HMGA1 knockdown resulted in mitotic chromosome segregation errors, causing micronuclei formation. However, we did not observe an increase in lagging chromosomes in *D1* mutant spermatogonia or HMGA1-depleted mouse cells (Figure 4 –figure supplement 1A-G), suggesting an alternative route for micronuclei formation. Instead, time-lapse live observation showed that micronuclei formed by budding off the interphase nucleus both in *Drosophila* spermatogonia and mouse cells (Figure 4A-D). In controls, nuclear contents (visualized by a GFP-tagged nuclear protein in *Drosophila* or the DNA dye, Hoechst, in

mouse cells) were maintained as a single and stable entity for a prolonged time period. In contrast, *D1* mutant and HMGA1-knockdown cells showed budding off of nuclear contents in interphase, leading to micronuclei formation. These results show that micronuclei in *D1* mutant/HMGA1-knockdown cells are generated during interphase, via budding from the nucleus.

D1 bundles satellite DNA from multiple chromosomes to form chromocenter

Based on the above results, we postulated that chromocenter formation, i.e. clustering of satellite DNA from multiple chromosomes, might be a mechanism to bundle heterologous chromosomes together to prevent individual chromosomes from floating out of nucleus. In this manner, the full set of chromosomes may be retained within a single nucleus. In the absence of chromocenter formation, individual chromosomes may bud off the nucleus, leading to micronuclei formation.

in vitro experiments indicated that HMGA1 is capable of crosslinking multiple DNA strands with individual AT-hooks binding AT-rich DNA strands (Vogel et al., 2011). Bundling of DNA in this manner by D1/HMGA1 could explain how pericentromeric satellite DNA from multiple chromosomes may be clustered to form chromocenters. A few lines of evidence support this idea. When *Drosophila* D1 was expressed in mouse cells, it localized to the chromocenter as described above (Figure 1G), and its overexpression enhanced chromocenter formation in a dose-dependent manner (Figure 5A-C): the higher amount D1 was expressed in mouse cells, the fewer chromocenters per cell was observed (i.e. more clustering). These results suggest that D1 is sufficient to bundle its binding target, tethering it to chromocenter. Consistent with this idea, we found that artificial tethering of D1 protein to euchromatic LacO repeat DNA sequences was sufficient to bring LacO repeats to the chromocenter. D1 protein or D1-LacI fusion protein was expressed in a *Drosophila* strain in which LacO repeats are inserted in the distal regions of the 2^{nd} chromosome (Figure 5D, arrows). In control spermatogonial cells expressing wild type D1, LacO repeats were observed far away from the $\{AATAT\}_n$ satellite foci/chromocenters (Figure 5E, G, arrow indicates site of LacO repeats in interphase nucleus). However, in cells expressing the LacI-D1 chimeric protein, we observed recruitment of the LacO repeats close to $\{AATAT\}_n$/chromocenters (Figure 5F, G, arrow indicates site of LacO repeats recruited to the

chromocenter), demonstrating that D1's binding to a DNA sequence is sufficient to incorporate the target sequence into chromocenters.

Although it cannot be visualized how DNA strands from multiple chromosome might be bundled in these interphase chromocenters, deconvolution microscopy of D1/HMGA1 proteins on early mitotic chromosomes revealed proteinaceous threads between individual chromosomes (Figure 6A, B, arrows indicate D1/HMGA1 threads connecting mitotic chromosomes), which we speculate contribute to bundling of chromosomes in interphase. These threads were also detectable by DNA FISH against $\{AATAT\}_n$ and major satellite (Figure 6C, D, dotted lines are alongside the satellite DNA threads), suggesting that satellite DNA bound by D1/HMGA1 can form threads that connect chromosomes. These D1/HMGA1 threads are reminiscent of 'DNA fibers', which were observed among mitotic chromosomes, although their function has never been appreciated (Burdick, 1976; Takayama, 1975; Kuznetsova et al., 2007).

Taken together, these results support a model, in which D1/HMGA1 bind their target sequences (satellite DNA) on multiple chromosomes and bundle them into chromocenters, likely via their multivalent DNA binding domains (multiple AT-hooks) (Figure 6E).

Discussion

The function of chromocenters, as well as that of satellite DNA, has remained enigmatic, even though cytological association of pericentromeric satellite DNA into chromocenters was identified almost 50 years ago (Pardue and Gall, 1970). Pericentromeric heterochromatin has most often been studied and discussed in the context of how to maintain its heterochromatic, repressed nature (Nishibuchi and Déjardin, 2017), based on the assumption that the underlying sequences are mostly selfish, which have negative phenotypic consequences when derepressed in cells (Zeller and Gasser, 2017).

Although satellite DNA's function has been speculated and implicated in several examples (Yunis and Yasmineh, 1971; Dernburg et al., 1996; Menon et al., 2014; Bonaccorsi et

al., 1990), the non-coding nature and lack of conservation in repeat sequence among closely related species led to the idea that they are mostly junk DNA, serving no essential function (Doolittle and Sapienza, 1980; Walker, 1971). Instead, we propose that satellite DNA is a critical constituent of eukaryotic chromosomes to ensure encapsulation of all chromosomes in interphase nucleus. Our results may also explain why the sequences of pericentromeric satellite DNA are so divergent among closely related species, a contributing factor that led to their dismissal as junk. Based on our model that pericentromeric satellite DNA serves as a platform for generating heterologous chromosome association to form chromocenters, the essential feature of satellite DNA is that they are bound by protein(s) capable of bundling multiple DNA strands. If so, the underlying sequence does not have to be conserved. Instead, the binding of satellite DNA by a chromocenter bundling protein may be a critical feature of pericentromeric satellite DNAs. Based on this idea, chromocenter bundling proteins and pericentromeric satellite DNA may be co-evolving.

In summary, our study provides the first evidence for a conserved function of pericentromeric satellite DNA and chromocenters. Our data suggest that the multi-AT hook proteins, D1 and HMGA1, play an evolutionarily conserved role in the formation of chromocenters, likely via their ability to bind and bundle satellite DNA from heterologous chromosomes. Heterologous chromosome association, mediated by chromocenter-binding proteins, may represent a third mode of chromosomal ‘gluing’ after meiotic homologous pairing and sister chromatid cohesion. Through heterologous association, the chromocenter plays a fundamental role in maintaining the full complement of the genome, which is divided into multiple chromosomes, into a single nucleus, thereby bringing about a signature characteristic of eukaryotic cells.

Acknowledgments:

We thank Cheng-Yu Lee, Scott Hawley, Stephen Weiss, Harry Mobley, Dave Bridges, Daniel Eitzman, Georg Krohne, Bloomington Drosophila Stock Center, Kyoto Stock Center, Developmental Studies Hybridoma Bank and Michigan Imaging Laboratory for reagents and resources. We thank the Yamashita lab members, Sue Hammoud, Ajit Joglekar, Puck Ohi, Dan

Barbash, and Maurizio Gatti for discussion and comments on the manuscript. This research was supported by the Howard Hughes Medical Institute (Y.Y) and an American Heart Association postdoctoral fellowship (M.J). MJ and YY conceived the project, interpreted the data and wrote the manuscript. All authors contributed to conducting experiments and analyzing data.

Materials and Methods:

Fly husbandry and strains. All fly stocks were raised on standard Bloomington medium at 25°C. The following fly stocks were used: $D1^{EY05004}$(BDSC17340), Df(3R)BSC666 (BDSC26518), *UAS-Omi*^{RNAi} (BDSC55165), *UAS-GFP-nls* (BDSC4776) and *UAS-GFP-ER-SR* (BDSC59042) were obtained from the Bloomington *Drosophila* stock center. $D1^{LL03310}$ (DGRC140754) and Df31-GFP (DGRC110806) were obtained from the Kyoto stock center. *nos-gal4*(Van Doren et al., 1998), *hs-flp;nos-FRT-stop-FRT-gal4,UAS-GFP* (Salzmann et al., 2013), *UAS-H2A-YFP* (Bellaïche et al., 2001) and *B1 LacO* (Vazquez et al., 2002) have been previously described. A stock containing B chromosomes, *mtrm*^{126}*+B* (Bauerly et al., 2014), was a kind gift from Scott Hawley. Chromocenter disruption was scored in Drosophila testes by assessing $\{AATAT\}_n$ morphology in GFP+ cells that were generated as follows in control (hs-flp; *nos-FRT-stop-FRT-gal4,UAS-GFP)* and *D1* mutant (*hs-flp;nos-FRT-stop-FRT-gal4, UAS-GFP*;$D1^{LL03310}$/*Df*) flies. Testes were dissected 24h following a 20 minute heat shock at 37°C. Micronuclei were scored in 0-3d testes where early germ cell chromosomes were labeled with H2A-YFP. The genotypes used were, control – *nos>H2A-YFP* and D1 mutant – *nos>H2A-YFP*; *D1LL03310/Df*.

Transgene construction. For construction of *UAS-GFP-D1*, the *D1* ORF was PCR-amplified from cDNA using the following primer pair, 5'-GATCAGATCTATGGAGGAAGTTGCGGTAAAG-3' and 5'-GATCCTCGAGTTAGGCAGCTACCGATTCGG-3'. The amplified fragment was subcloned into the BglII and XhoI sites of *pUASt-EGFP-attB*(Salzmann et al., 2013) resulting in *UAS-GFP-D1*. For *UAS-GFP-LacI-D1*, the *LacI* ORF (lacking 11 C-terminal residues) (Straight et al., 1996) was synthesized using GeneArt (Thermofisher) and inserted into the BglII site of *UAS-GFP-D1* resulting in *UAS-GFP-LacI-D1*. Transgenic flies were generated by PhiC31 integrase-

mediated transgenesis into the *attP40* site (BestGene). For expression of GFP and GFP-D1 in mouse cells, *GFP* and *GFP-D1* was subcloned from *pUASt-EGFP-attB* into pCDNA3 (gift from Cheng-Yu Lee) using EcoRI and XhoI sites.

Cell lines. MOVAS cells were obtained from Daniel Eitzman. C2C12 cells were obtained from David Bridges. RAW264.7 cells were obtained from Dr. Harry Mobley. C3H10T1/2 cells were obtained from Stephen Weiss. MOVAS, C2C12 and RAW264.7 cells were maintained in Dulbecco's minimal essential medium (DMEM) (Gibco) supplemented with 10% fetal bovine serum (FBS). C3H10T1/2 cell line was maintained in alpha minimal essential media (Gibco) supplemented with 10% fetal bovine serum.

siRNA and Transfections. RNA interference (RNAi) against HMGA1 was performed using ON-TARGET plus Mouse HMGA1 siRNA SMARTpool (Dharmacon, L-049293-01) consisting of the following target sequences, CCAUUUAGCCGCAGCCCGA, AGGCAAACGGGCACCAACA, GGGCGCAGCAGACUGGUUA, GUUCAUUCUUAGAUACCCA. ON-TARGET plus Non-targeting pool (Dharmacon, D-001810-10) consisting of the following sequences, UGGUUUACAUGUCGACUAA, UGGUUUACAUGUUGUGUGA, UGGUUUACAUGUUUUCUGA, UGGUUUACAUGUUUUCCUA, was used as a negative control. siRNA transfections were performed using DharmaFECT 4 reagent (Dharmacon) according to the manufacturer's protocol. 25nM of siControl and siHMGA1 were transfected using DharmaFECT 4 (Dharmacon) according to the manufacturer’s protocol. Cells were fixed for immunostaining/*in situ* hybridization 6 days post transfection. Transient transfection of GFP and GFP-D1 was performed using Fugene HD (Roche) reagent according to the manufacturer’s protocol.

Immunofluorescence staining and microscopy. For *Drosophila* tissues, immunofluorescence staining was performed as described previously(Cheng et al., 2008). Briefly, tissues were dissected in PBS, transferred to 4% formaldehyde in PBS and fixed for 30 minutes. Testes were then washed in PBS-T (PBS containing 0.1% Triton-X) for at least 60 minutes, followed by

315 incubation with primary antibody in 3% bovine serum albumin (BSA) in PBS-T at 4°C
316 overnight. Samples were washed for 60 minutes (three 20-minute washes) in PBS-T, incubated
317 with secondary antibody in 3% BSA in PBS-T at 4°C overnight, washed as above, and mounted
318 in VECTASHIELD with DAPI (Vector Labs). The following primary antibodies were used:
319 rabbit anti-vasa (1:200; d-26; Santa Cruz Biotechnology), rabbit anti-H3K9 dimethyl (1:200;
320 Abcam, ab32521), guinea pig anti-Otefin (gift from Georg Krohne, 1:400), chicken anti-Cid
321 (1:500, generated using the synthetic peptide CDGENDANDGYVSDNYNDSESVAA
322 (Covance)), mouse anti-LaminDm$_0$ (ADL84.12, 1:200, Developmental Studies Hybridoma
323 Bank), mouse anti-γ–H2Av (UNC93-5.2.1, 1:400, Developmental Studies Hybridoma Bank),
324 Phalloidin-Alexa546 (ThermoFisher, a22283, 1:200). Adherent mouse cells were fixed in 4%
325 formaldehyde in PBS for 20 minutes at room temperature on coverslips. Cells were
326 permeabilized in PBS-T for 5 minutes, rinsed 3 times with PBS, blocked using 3% BSA in PBS-
327 T for 30 minutes at room temperature and incubated with primary antibody diluted in 3% BSA in
328 PBS-T overnight at 4°C. Cells were then washed for 30 minutes (three 10-minute washes),
329 incubated with secondary antibody in 3% BSA in PBS-T for 2 hours at room temperature,
330 washed as above and mounted in VECTASHIELD with DAPI (Vector Labs). For nucleosolic
331 extraction, cells were incubated with CSK buffer (10mM PIPES pH7, 100mM NaCl, 300mM
332 sucrose, 3mM $MgCl_2$, 0.5% Triton X-100, 1mM PMSF) for 10 minutes at room temperature.
333 After CSK extraction, cells were washed with PBS and fixed and immunostained as above. The
334 following antibodies were used: rabbit anti-HMGA1 (1:400, Abcam, ab129153), goat anti-
335 LaminB (C-20) (1:20, Santa Cruz Biotechnology, sc-2616), mouse anti-α-tubulin (4.3, 1:100,
336 Developmental Studies Hybridoma Bank) and γ–H2Ax S139 (2577, 1:200, Cell Signaling
337 Technologies). Images were taken using a Leica TCS SP8 confocal microscope with 63x oil-
338 immersion objectives (NA=1.4). Deconvolution was performed when indicated using the
339 Hyvolution package from Leica. Images were processed using Adobe Photoshop software.

340

341 **Time-lapse live imaging.** Testes from newly eclosed flies were dissected into
342 Schneider's *Drosophila* medium containing 10% fetal bovine serum. The testis tips were placed
343 inside a sterile glass-bottom chamber and were mounted on a three-axis computer-controlled
344 piezoelectric stage. An inverted Leica TCS SP8 confocal microscope with a 63× oil immersion

objective (NA = 1.4) was used for imaging. For mouse live cell imaging, transfected cells were seeded onto a sterile glass-bottom chamber coated with poly-lysine. Cells were incubated with Hoechst 33342 for 10 minutes, rinsed with PBS and fresh medium was added to the chamber. Cells were imaged using a stage-top Tokai-Hit incubator that was mounted on an inverted TCS SP5 confocal microscope with a 63x oil immersion objective (NA = 1.4). All images were processed using Adobe Photoshop software.

DNA fluorescence *in situ* hybridization. Whole mount *Drosophila* testes were prepared as described above, and optional immunofluorescence staining protocol was carried out first. Subsequently, samples were post-fixed with 4% formaldehyde for 10 minutes and washed in PBS-T for 30 minutes. Fixed samples were incubated with 2 mg/ml RNase A solution at 37°C for 10 minutes, then washed with PBS-T + 1mM EDTA. Samples were washed in 2xSSC-T (2xSSC containing 0.1% Tween-20) with increasing formamide concentrations (20%, 40% and 50%) for 15 minutes each followed by a final 30-minute wash in 50% formamide. Hybridization buffer (50% formamide, 10% dextran sulfate, 2x SSC, 1mM EDTA, 1 µM probe) was added to washed samples. Samples were denatured at 91°C for 2 minutes, then incubated overnight at 37°C. For mitotic chromosome spreads, testes and larval 3rd instar brains were squashed according to previously described methods (Larracuente and Ferree, 2015). Briefly, tissue was dissected into 0.5% sodium citrate for 5-10 minutes and fixed in 45% acetic acid/2.2% formaldehyde for 4-5 minutes. Fixed tissues were firmly squashed with a cover slip and slides were submerged in liquid nitrogen until bubbling ceased. Coverslips were then removed with a razor blade and slides were dehydrated in 100% ethanol for at least 5 minutes. After drying, hybridization mix (50% formamide, 2x SSC, 10% dextran sulfate, 100 ng of each probe) was applied directly to the slide, samples were heat denatured at 95°C for 5 minutes and allowed to hybridize overnight at room temperature. Following hybridization, slides were washed 3 times for 15 minutes in 0.2X SSC and mounted with VECTASHIELD with DAPI (Vector Labs). For the *in situ* experiment described in Figure 4j-m, testes were dissected into PBS and fixed in 4% formaldehyde for 4 minutes. Tips of fixed testes were firmly squashed with a cover slip and slides were submerged in liquid nitrogen until bubbling ceased. Coverslips were removed with a razor blade and slides were subjected to 5-minute washes in 2XSSC and 2XSSC with 0.1% Tween-20. The samples were denatured in freshly made 0.07N NaOH for 5 minutes, rinsed in

2X SSC. Hybridization mix (50% formamide, 2x SSC, 10% dextran sulfate, 100 ng of each probe) was added directly to the slide and allowed to hybridize overnight at room temperature. Following hybridization, slides were washed 3 times for 15 minutes in 0.2X SSC and mounted with VECTASHIELD with DAPI (Vector Labs). The following probes were used for *Drosophila* in situ hybridization: $\{AATAT\}_6$, $\{AAGAG\}_6$, IGS and have been previously described. LacO probe - 5'-Cy5-CCACAAATTGTTATCCGCTCACAATTCCAC-3'. For interphase mouse cells, optional immunostaining was carried out as above. Subsequently, samples were post-fixed with 4% formaldehyde in PBS for 10 minutes and rinsed three times in PBS. Post-fixed cells were incubated with 0.1 mg/ml RNase A solution at 37°C for 1 hour, rinsed three times in PBS and denatured in 1.9M HCl for 30 minutes. After three rinses in ice-cold PBS, hybridization mix (2X SSC, 60% formamide, 5µg/ml salmon sperm DNA and 500nM probe) was added to the samples and incubated overnight at room temperature. Following hybridization, coverslips were washed 3 times for 15 minutes in 2X SSC and mounted with VECTASHIELD with DAPI (Vector Labs). For mouse mitotic cells, chromosomes were spread on slides as previously described. Subsequently, chromosomes were denatured in 70% formamide in 2XSSC for 1.5 minutes at 70°C, dehydrated in 100% ethanol and hybridization mix (2X SSC, 60% formamide, 5µg/ml salmon sperm DNA and 500nM probe) was added directly to the slide and incubated overnight at room temperature. Following hybridization, slides were washed 3 times for 15 minutes in 2X SSC and mounted with VECTASHIELD with DAPI (Vector Labs). The following probe was used: Major satellite - 5'-Cy3-GGAAAATTTAGAAATGTCCACTG-3'.

References:

Barton, L.J., S.R. Wilmington, M.J. Martin, H.M. Skopec, K.E. Lovander, B.S. Pinto, and P.K. Geyer. 2014. Unique and Shared Functions of Nuclear Lamina LEM Domain Proteins in Drosophila. *Genetics*. 197:653–665. doi:10.1534/genetics.114.162941.

Bauerly, E., S.E. Hughes, D.R. Vietti, D.E. Miller, W. McDowell, and R.S. Hawley. 2014. Discovery of supernumerary B chromosomes in Drosophila melanogaster. *Genetics*. 196:1007–16. doi:10.1534/genetics.113.160556.

Bellaïche, Y., M. Gho, J.A. Kaltschmidt, A.H. Brand, and F. Schweisguth. 2001. Frizzled regulates localization of cell-fate determinants and mitotic spindle rotation during asymmetric cell division. *Nat. Cell Biol.* 3:50–7. doi:10.1038/35050558.

Bonaccorsi, S., M. Gatti, C. Pisano, and A. Lohe. 1990. Transcription of a satellite DNA on two Y chromosome loops of Drosophila melanogaster. *Chromosoma*. 99:260–6. doi:10.1007/BF01731701.

Bulut-Karslioglu, A., V. Perrera, M. Scaranaro, I.A. de la Rosa-Velazquez, S. van de Nobelen, N. Shukeir, J. Popow, B. Gerle, S. Opravil, M. Pagani, S. Meidhof, T. Brabletz, T. Manke, M. Lachner, and T. Jenuwein. 2012. A transcription factor-based mechanism for mouse heterochromatin formation. *Nat. Struct. Mol. Biol.* 19:1023–30. doi:10.1038/nsmb.2382.

Burdick, A.B. 1976. Somatic cell chromosome interconnections in trypan preparations of Chinese hamster testicular cells. *Exp. Cell Res.* 99:425–8.

Cheng, J., N. Türkel, N. Hemati, M.T. Fuller, A.J. Hunt, and Y.M. Yamashita. 2008. Centrosome misorientation reduces stem cell division during ageing. *Nature*. 456:599–604. doi:10.1038/nature07386.

Crasta, K., N.J. Ganem, R. Dagher, A.B. Lantermann, E.V. Ivanova, Y. Pan, L. Nezi, A. Protopopov, D. Chowdhury, and D. Pellman. 2012. DNA breaks and chromosome pulverization from errors in mitosis. *Nature*. 482:53–8. doi:10.1038/nature10802.

Denais, C.M., R.M. Gilbert, P. Isermann, A.L. McGregor, M. te Lindert, B. Weigelin, P.M. Davidson, P. Friedl, K. Wolf, and J. Lammerding. 2016. Nuclear envelope rupture and repair during cancer cell migration. *Science*. 352:353–8. doi:10.1126/science.aad7297.

Dernburg, A.F., J.W. Sedat, and R.S. Hawley. 1996. Direct evidence of a role for heterochromatin in meiotic chromosome segregation. *Cell*. 86:135–46.

Doolittle, W.F., and C. Sapienza. 1980. Selfish genes, the phenotype paradigm and genome evolution. *Nature*. 284:601–3.

Doren, M. Van, A.L. Williamson, and R. Lehmann. 1998. Regulation of zygotic gene expression in Drosophila primordial germ cells. *Curr. Biol.* 8:243–6.

Dorn, G.W., C.F. Clark, W.H. Eschenbacher, M.-Y.Y. Kang, J.T. Engelhard, S.J. Warner, S.J. Matkovich, and C.C. Jowdy. 2011. MARF and Opa1 control mitochondrial and cardiac function in Drosophila. *Circ. Res.* 108:12–7. doi:10.1161/CIRCRESAHA.110.236745.

Fransz, P., J.H. De Jong, M. Lysak, M.R. Castiglione, and I. Schubert. 2002. Interphase chromosomes in Arabidopsis are organized as well defined chromocenters from which euchromatin loops emanate. *Proc. Natl. Acad. Sci. U.S.A.* 99:14584–9. doi:10.1073/pnas.212325299.

Goodwin, G.H., C. Sanders, and E.W. Johns. 1973. A new group of chromatin-associated proteins with a high content of acidic and basic amino acids. *Eur. J. Biochem.* 38:14–9.

Guenatri, M., D. Bailly, C. Maison, and G. Almouzni. 2004. Mouse centric and pericentric satellite repeats form distinct functional heterochromatin. *J. Cell Biol.* 166:493–505. doi:10.1083/jcb.200403109.

Hahn, M., S. Dambacher, S. Dulev, A. Kuznetsova, S. Eck, S. Worz, D. Sadic, M. Schulte, J. Mallm, A. Maiser, P. Debs, H. Melchner, H. Leonhardt, L. Schermelleh, K. Rohr, K. Rippe, Z. Storchova, and G. Schotta. 2013. Suv4-20h2 mediates chromatin compaction and is important for cohesin recruitment to heterochromatin. *Genes & Development*. 27:859872. doi:10.1101/gad.210377.112.

Hatch, E.M., A.H. Fischer, T.J. Deerinck, and M.W. Hetzer. 2013. Catastrophic nuclear envelope collapse in cancer cell micronuclei. *Cell*. 154:47–60. doi:10.1016/j.cell.2013.06.007.

Hatch, E.M., and M.W. Hetzer. 2015. Chromothripsis. *Curr. Biol.* 25:R397–9. doi:10.1016/j.cub.2015.02.033.

Jagannathan, M., N. Warsinger-Pepe, G.J. Watase, and Y.M. Yamashita. 2017. Comparative Analysis of Satellite DNA in the Drosophila melanogaster Species Complex. *G3 (Bethesda)*. 7:693–704. doi:10.1534/g3.116.035352.

Kuznetsova, I.S., N.I. Enukashvily, E.M. Noniashvili, A.N. Shatrova, N.D. Aksenov, V.V. Zenin, A.P. Dyban, and O.I. Podgornaya. 2007. Evidence for the existence of satellite DNA-containing connection between metaphase chromosomes. *J. Cell. Biochem.*

101:1046–61. doi:10.1002/jcb.21237.

Levinger, L., and A. Varshavsky. 1982a. Selective arrangement of ubiquitinated and D1 protein-containing nucleosomes within the Drosophila genome. *Cell*. 28:375–85.

Levinger, L., and A. Varshavsky. 1982b. Protein D1 preferentially binds A + T-rich DNA in vitro and is a component of Drosophila melanogaster nucleosomes containing A + T-rich satellite DNA. *Proc. Natl. Acad. Sci. U.S.A.* 79:7152–6.

Lund, T., J. Holtlund, M. Fredriksen, and S.G. Laland. 1983. On the presence of two new high mobility group-like proteins in HeLa S3 cells. *FEBS Lett.* 152:163–7.

Lyon, MF, and AG Searle. 1989. Genetic variants and strains of the laboratory mouse.

Menon, D.U., C. Coarfa, W. Xiao, P.H. Gunaratne, and V.H. Meller. 2014. siRNAs from an X-linked satellite repeat promote X-chromosome recognition in Drosophila melanogaster. *Proc. Natl. Acad. Sci. U.S.A.* 111:16460–5. doi:10.1073/pnas.1410534111.

Nishibuchi, G., and J. Déjardin. 2017. The molecular basis of the organization of repetitive DNA-containing constitutive heterochromatin in mammals. *Chromosome Res.* 25:77–87. doi:10.1007/s10577-016-9547-3.

Pardue, M.L., and J.G. Gall. 1970. Chromosomal localization of mouse satellite DNA. *Science*. 168:1356–8.

Peters, A.H., D. O'Carroll, H. Scherthan, K. Mechtler, S. Sauer, C. Schöfer, K. Weipoltshammer, M. Pagani, M. Lachner, A. Kohlmaier, S. Opravil, M. Doyle, M. Sibilia, and T. Jenuwein. 2001. Loss of the Suv39h histone methyltransferases impairs mammalian heterochromatin and genome stability. *Cell*. 107:323–37.

Pinheiro, I., R. Margueron, N. Shukeir, M. Eisold, C. Fritzsch, F.M. Richter, G. Mittler, C. Genoud, S. Goyama, M. Kurokawa, J. Son, D. Reinberg, M. Lachner, and T. Jenuwein. 2012. Prdm3 and Prdm16 are H3K9me1 methyltransferases required for mammalian heterochromatin integrity. *Cell*. 150:948–60. doi:10.1016/j.cell.2012.06.048.

Probst, A.V., I. Okamoto, M. Casanova, F. El Marjou, P. Le Baccon, and G. Almouzni. 2010. A strand-specific burst in transcription of pericentric satellites is required for chromocenter formation and early mouse development. *Dev. Cell*. 19:625–38. doi:10.1016/j.devcel.2010.09.002.

Raab, M., M. Gentili, H. de Belly, H.R. Thiam, P. Vargas, A.J. Jimenez, F. Lautenschlaeger, R. Voituriez, A.M. Lennon-Duménil, N. Manel, and M. Piel. 2016. ESCRT III repairs

nuclear envelope ruptures during cell migration to limit DNA damage and cell death. *Science*. 352:359–62. doi:10.1126/science.aad7611.

Radic, M.Z., M. Saghbini, T.S. Elton, R. Reeves, and B.A. Hamkalo. 1992. Hoechst 33258, distamycin A, and high mobility group protein I (HMG-I) compete for binding to mouse satellite DNA. *Chromosoma*. 101:602–8.

Rodriguez Alfageme, C., G.T. Rudkin, and L.H. Cohen. 1980. Isolation, properties and cellular distribution of D1, a chromosomal protein of Drosophila. *Chromosoma*. 78:1–31.

Salzmann, V., M. Inaba, J. Cheng, and Y.M. Yamashita. 2013. Lineage tracing quantification reveals symmetric stem cell division in Drosophila male germline stem cells. *Cell Mol Bioeng*. 6:441–448. doi:10.1007/s12195-013-0295-6.

Straight, A.F., A.S. Belmont, C.C. Robinett, and A.W. Murray. 1996. GFP tagging of budding yeast chromosomes reveals that protein-protein interactions can mediate sister chromatid cohesion. *Curr. Biol.* 6:1599–608.

Strauss, F., and A. Varshavsky. 1984. A protein binds to a satellite DNA repeat at three specific sites that would be brought into mutual proximity by DNA folding in the nucleosome. *Cell*. 37:889–901.

Sun, X., H.D. Le, J.M. Wahlstrom, and G.H. Karpen. 2003. Sequence analysis of a functional Drosophila centromere. *Genome Res.* 13:182–94. doi:10.1101/gr.681703.

Sun, X., J. Wahlstrom, and G. Karpen. 1997. Molecular structure of a functional Drosophila centromere. *Cell*. 91:1007–19.

Takayama, S. 1975. Interchromosomal connectives in squash preparations of L cells. *Exp. Cell Res.* 91:408–12.

Vazquez, J., A.S. Belmont, and J.W. Sedat. 2002. The dynamics of homologous chromosome pairing during male Drosophila meiosis. *Curr. Biol.* 12:1473–83.

Vogel, B., A. Löschberger, M. Sauer, and R. Hock. 2011. Cross-linking of DNA through HMGA1 suggests a DNA scaffold. *Nucleic Acids Res.* 39:7124–33. doi:10.1093/nar/gkr396.

Walker, P.M. 1971. Origin of satellite DNA. *Nature*. 229:306–8.

Willard, H.F. 1990. Centromeres of mammalian chromosomes. *Trends Genet.* 6:410–6.

Yacobi-Sharon, K., Y. Namdar, and E. Arama. 2013. Alternative germ cell death pathway in Drosophila involves HtrA2/Omi, lysosomes, and a caspase-9 counterpart. *Dev. Cell*.

522 25:29–42. doi:10.1016/j.devcel.2013.02.002.
523 Yunis, J.J., and W.G. Yasmineh. 1971. Heterochromatin, satellite DNA, and cell function.
524 Structural DNA of eucaryotes may support and protect genes and aid in speciation.
525 *Science*. 174:1200–9. doi:10.1126/science.174.4015.1200.
526 Zeller, P., and S.M. Gasser. 2017. The Importance of Satellite Sequence Repression for Genome
527 Stability. *Cold Spring Harb. Symp. Quant. Biol.* doi:10.1101/sqb.2017.82.033662.
528 Zeller, P., J. Padeken, R. van Schendel, V. Kalck, M. Tijsterman, and S.M. Gasser. 2016.
529 Histone H3K9 methylation is dispensable for Caenorhabditis elegans development but
530 suppresses RNA:DNA hybrid-associated repeat instability. *Nat. Genet.* 48:1385–1395.
531 doi:10.1038/ng.3672.
532 Zhang, C.-Z.Z., A. Spektor, H. Cornils, J.M. Francis, E.K. Jackson, S. Liu, M. Meyerson, and D.
533 Pellman. 2015. Chromothripsis from DNA damage in micronuclei. *Nature*. 522:179–84.
534 doi:10.1038/nature14493.
535 Zhu, Q., G.M. Pao, A.M. Huynh, H. Suh, N. Tonnu, P.M. Nederlof, F.H. Gage, and I.M. Verma.
536 2011. BRCA1 tumour suppression occurs via heterochromatin-mediated silencing.
537 *Nature*. 477:179–84. doi:10.1038/nature10371.
538
539

Figures

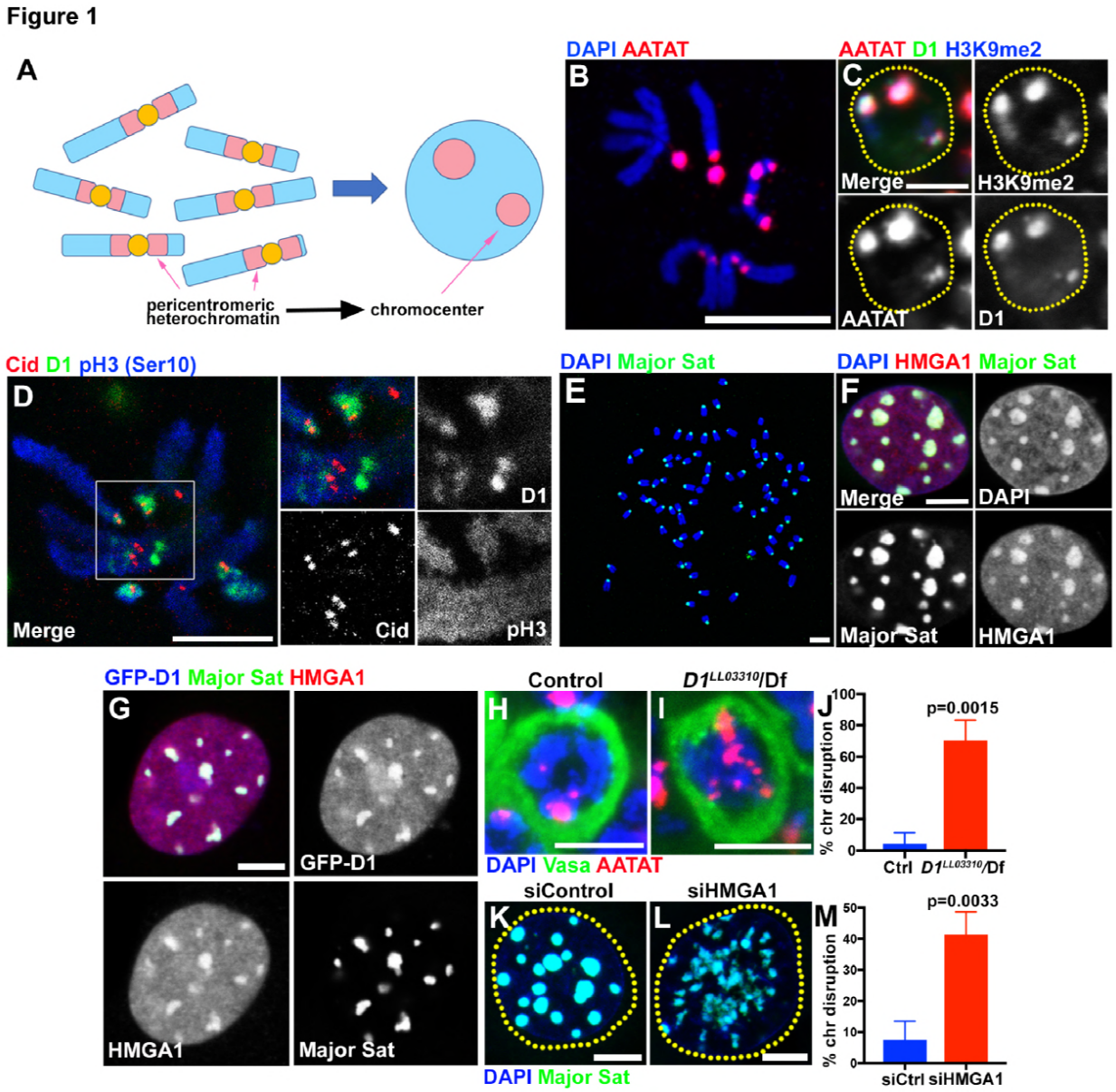

Figure 1. Multi-AT-hook proteins, D1 and HMGA1, are required for chromocenter formation in *Drosophila* and mouse cells.

(A) Schematic of pericentromeric heterochromatin being organized into chromocenter. (B) FISH against $\{AATAT\}_n$ satellite (red) on the *Drosophila* neuroblast mitotic chromosomes co-stained with DAPI (blue) indicating the location of $\{AATAT\}_n$ in the *Drosophila* genome. (C) FISH against $\{AATAT\}_n$ satellite (red) in spermatogonial cells immunostained for H3K9me2 (blue) and D1 (green). Dotted lines indicate nucleus. Bars: 5µm. (D) *Drosophila* neuroblast mitotic

549 chromosomes stained for D1 (green), phospho-histone H3 Serine 10 (pH3-S10) (blue) and
550 Cid/CENP-A (red). (E-G) FISH against the mouse major satellite (green) on C2C12 mitotic
551 chromosomes co-stained with DAPI (blue) (E), in interphase MOVAS cells co-stained for DAPI
552 (blue) and HMGA1 (red) (F) and in MOVAS cells expressing GFP-D1 (green) stained for
553 HMGA1 (red) (G). (H, I) FISH against $\{AATAT\}_n$ satellite (red) in control ($D1^{LL03310}$/+) (H) and
554 $D1^{LL03310}$/*Df* (I) spermatogonial cells stained for DAPI (blue) and Vasa (green). (J)
555 Quantification of spermatogonial cells with disrupted chromocenters (+/+ control n=117,
556 $D1^{LL03310}$/*Df* n=89) from three independent experiments. P value from student's t-test is shown.
557 Error bars: SD. (K, L) FISH against the major satellite (green) in siControl (K) and siHMGA1
558 (L) transfected MOVAS cells co-stained with DAPI (blue). (M) Quantification of cells with
559 disrupted chromocenters from siControl (n=304) and siHMGA1 (n=329) from three independent
560 experiments.
561

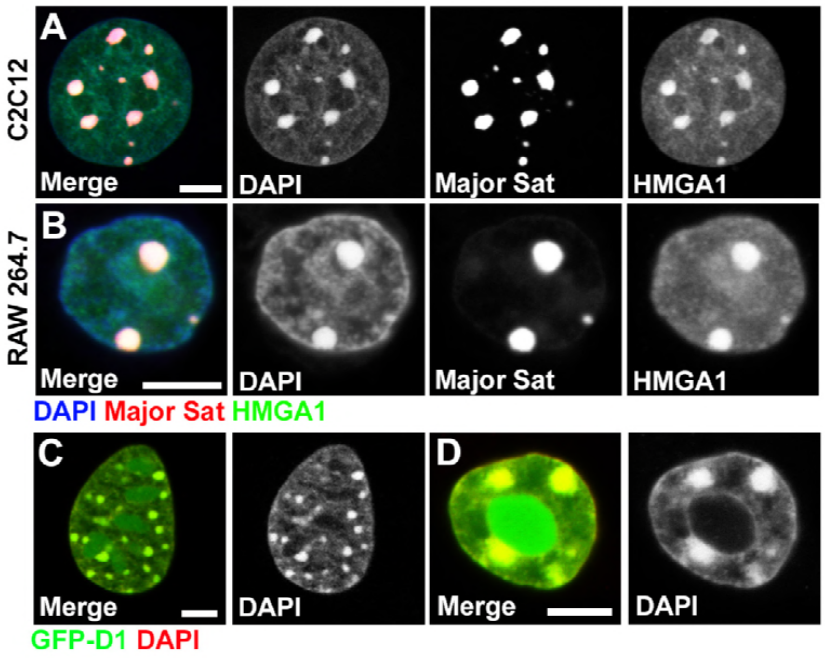

Figure 1- figure supplement 1. AT-hook containing proteins, *Drosophila* D1 and mouse HMGA1, localize to chromocenters in various mouse cell types.

(A, B) FISH against the mouse major satellite (red) in C2C12 (A) and RAW 264.7 (B) cells stained for HMGA1 (green) and DAPI (blue). (C, D) Colocalization of GFP-D1 (green) with DAPI-dense chromocenters in C2C12 (C) and RAW 264.7(D) cells. DAPI (red). Scale bars: 5μm.

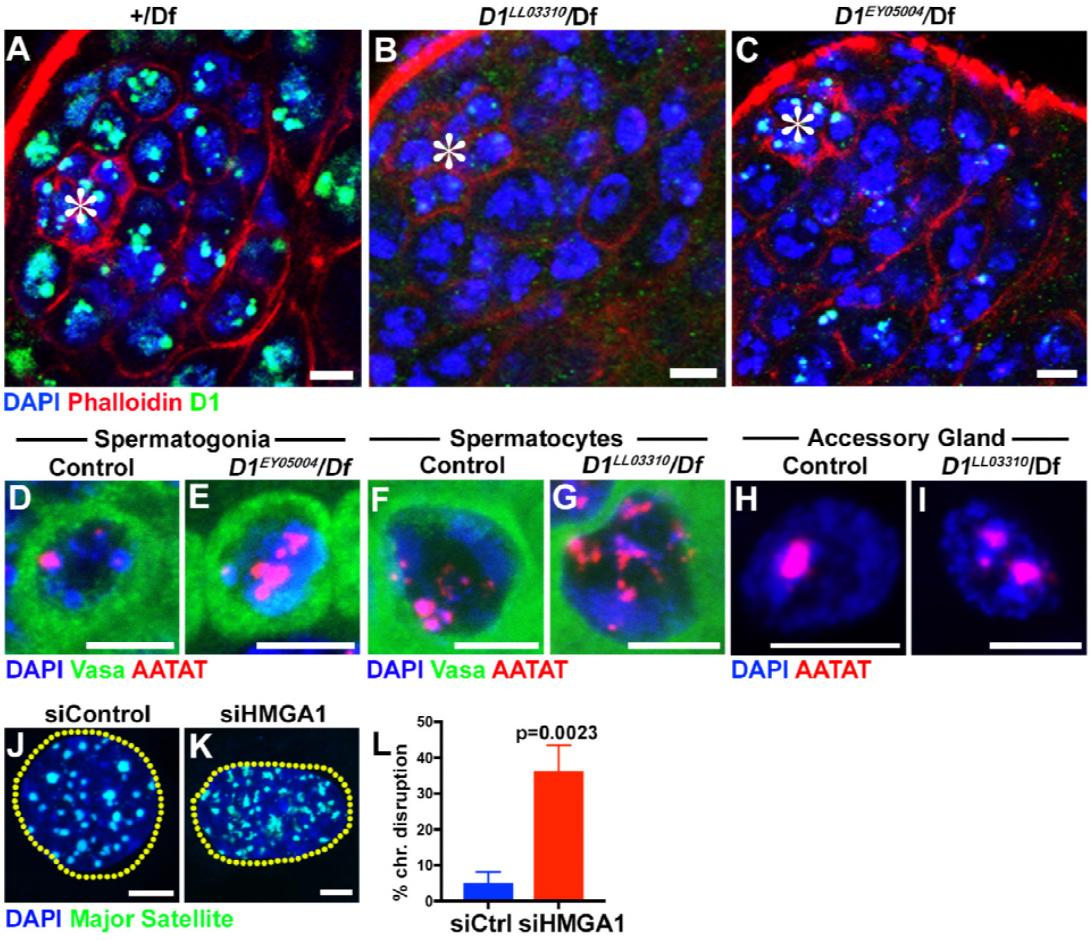

Figure 1- figure supplement 2. *Drosophila* D1 and mouse HMGA1 are required for chromocenter formation.

(A-C) Testes from control (+/*Df*) (A) and two *D1* mutant ($D1^{LL03310}$/*Df* (B)and $D1^{EY05004}$/*Df* (C)) flies were stained for DAPI (blue), Phalloidin (red) and D1 (green). Asterisks indicate the apical tip of the testis. Bars: 5µm. (D, E) FISH against $\{AATAT\}_n$ (red) in control ($D1^{EY05004}$/+) (D) and $D1^{EY05004}$/*Df* (E) spermatogonial cells stained for DAPI (blue) and Vasa (green). Bars: 2.5µm. (F, G) FISH against $\{AATAT\}_n$ (red) in control ($D1^{LL03310}$/+) (F) and $D1^{LL03310}$/*Df* (G) spermatocytes stained for DAPI (blue) and Vasa (green). (H, I) FISH against $\{AATAT\}_n$ (red) in control ($D1^{LL03310}$/+) (H) and $D1^{LL03310}$/*Df* (I) accessory gland cells stained for DAPI (blue). Bars: 5µm. (J, K) FISH against the major satellite (green) in siControl (J) and siHMGA1 transfected (K) C2C12 cells. Dotted lines indicate nucleus. (L) Quantification of cells with disrupted chromocenters in siControl (n=304) and siHMGA1 (n=298) transfected C2C12 cells from three independent experiments. P value from student's t-test is shown. Error bars: SD.

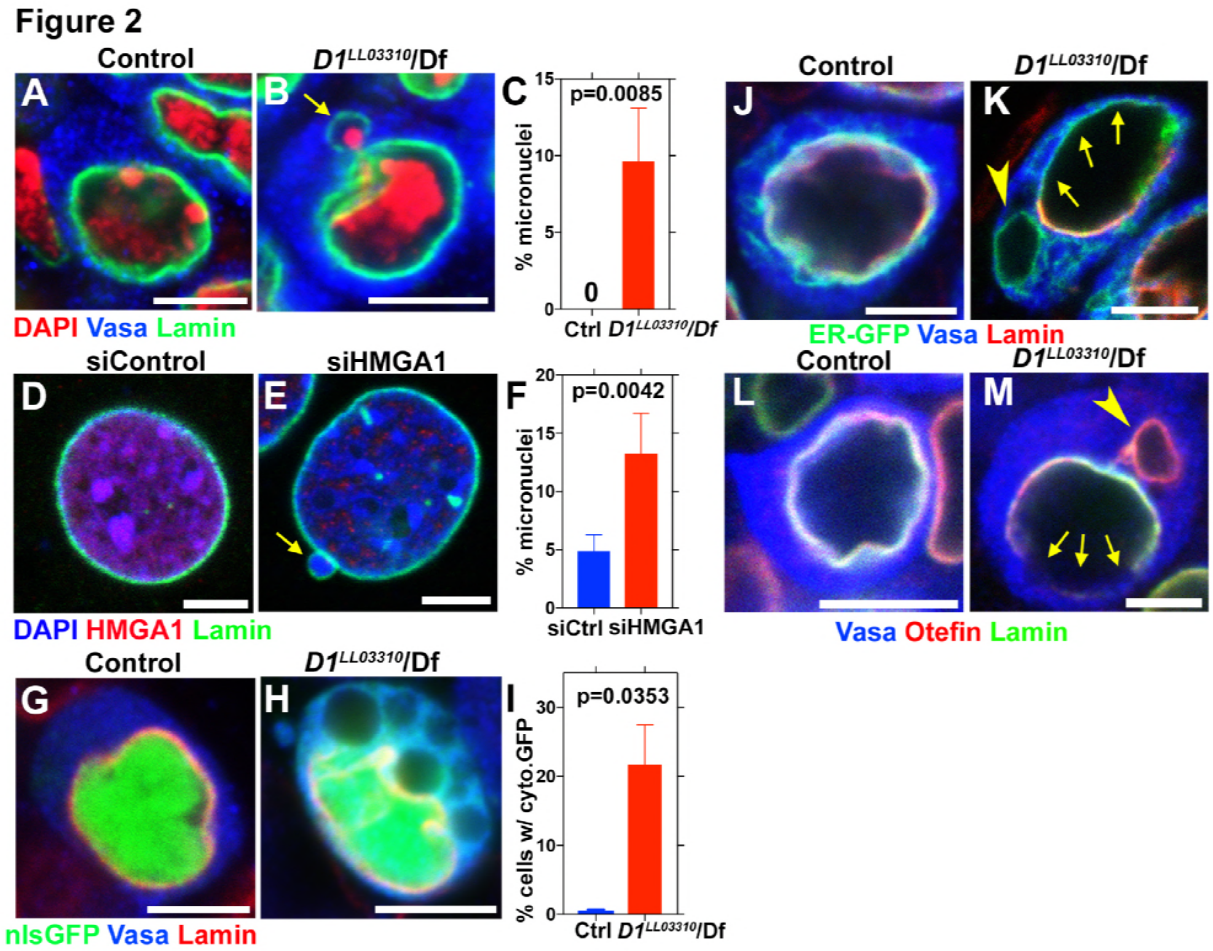

Figure 2. D1/HMGA1 loss of function results in micronuclei formation, and defective nuclear envelope integrity.

(A, B) Control (*D1*^{LL03310}/+) (A) and *D1*^{LL03310}/*Df* mutant (B) spermatogonial cells stained for DAPI (red), Vasa (blue) and LaminDm$_0$ (green). Arrow indicates micronucleus. Bars: 5μm. (C) Quantification of micronuclei containing cells from +/+ control (n=269) and *D1*^{LL03310}/*Df* (n=334) from three independent experiments. P value from student's t-test is shown. Error bars: SD. (D, E) siControl (D) and siHMGA1 transfected (E) MOVAS cells stained for DAPI (blue), HMGA1 (red) and Lamin (green). Arrow indicates micronucleus. (F) Quantification of micronuclei containing cells in siControl (n=518) and siHMGA1 (n=588) transfected cells from four independent experiments. (G, H) Control (*D1*^{LL03310}/+) (G) and *D1*^{LL03310}/*Df* (H) spermatogonia expressing nls-GFP (green) stained for Vasa (blue) and LaminDm$_0$ (red). nlsGFP was observed in cytoplasm in *D1*^{LL03310}/*Df* spermatogonia. (I) Quantification of spermatogonia

596 with cytoplasmic GFP (>1μm exclusions or pan-cytoplasmic) in $D1^{LL03310}$/+ (n=810) and
597 $D1^{LL03310}$/*Df* (n=780) testes from two independent experiments. (J, K) $D1^{LL03310}$/+ (J) and
598 $D1^{LL03310}$/*Df* (K) spermatogonia expressing ER-GFP marker (green) stained for Vasa (blue) and
599 $LaminDm_0$ (red). Arrowhead points to ER marker-positive micronucleus. Arrows point to site of
600 weak nuclear $LaminDm_0$ staining. (L, M) Control ($D1^{LL03310}$/+) (L) and $D1^{LL03310}$/*Df* (M)
601 spermatogonia stained for Vasa (blue) and $LaminDm_0$ (green) and Otefin (red). Arrowhead
602 points to Otefin-containing micronucleus. Arrows point to site of weak nuclear $LaminDm_0$
603 staining.
604

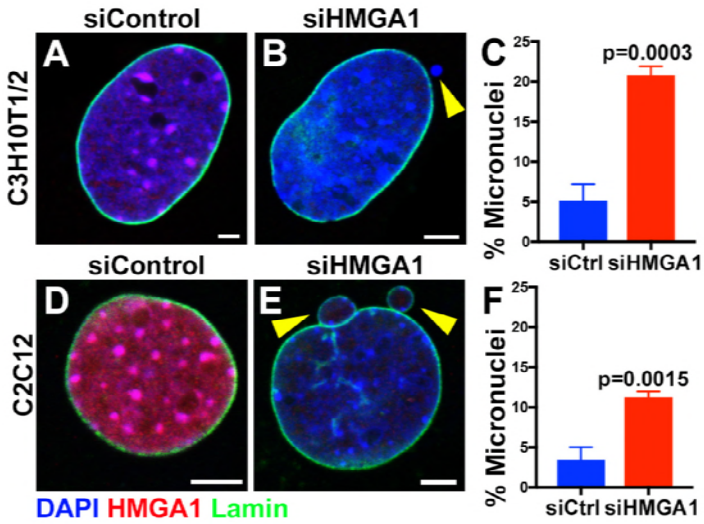

605

606 **Figure 2 –figure supplement 1. Formation of micronuclei upon chromocenter disruption in**
607 **C3H10T1/2 and C2C12 mouse cells.**

608 (A, B) siControl (A) and siHMGA1 (B) transfected C3H10T1/2 cells stained for DAPI (blue),
609 HMGA1 (red) and LaminB (green). Arrowhead indicates micronuclei. Bars: 5µm. (C)
610 Quantification of micronuclei containing cells from siControl (n=291) and siHMGA1 (n=303)
611 transfected cells from three independent experiments. P value from student's t-test is shown.
612 Error bars are SD. (D, E) siControl (D) and siHMGA1 (E) transfected C2C12 cells stained for
613 DAPI (blue), HMGA1 (red) and LaminB (green). Arrowhead indicates micronuclei. Bars: 5µm.
614 (F) Quantification of micronuclei containing cells from siControl (n=953) and siHMGA1
615 (n=699) transfected cells from three independent experiments. P value from student's t-test is
616 shown. Error bars are SD.

617

Figure 3

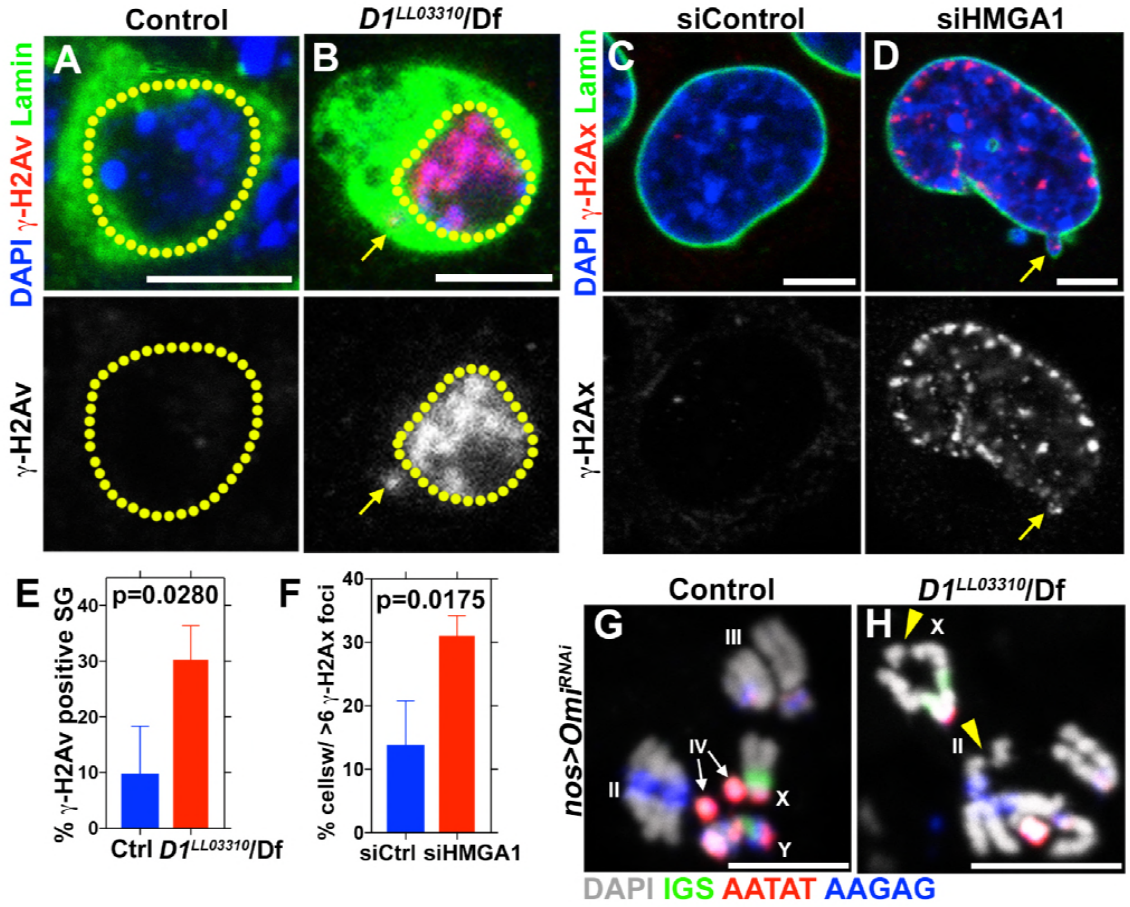

Figure 3. D1 mutation/HMGA1 depletion leads to an increase in DNA damage.

(A, B) Control (*D1*^{LL03310}/+) (A) and *D1*^{LL03310}/*Df* (B) spermatogonia stained for DAPI (blue), Vasa (green) and γ-H2Av (red). Dotted lines indicate nucleus and arrow points to DNA damage in micronuclei. (C, D) siControl (C) and siHMGA1 (D) transfected MOVAS cells stained for DAPI (blue), γ-H2Av (red) and LaminDm$_0$ (green). Arrow points to DNA damage in micronuclei. (E) Quantification of γ-H2Av positive cells in *D1*^{LL03310}/+ (n=317) and *D1*^{LL03310}/Df (n=242) spermatogonia from three independent experiments. (F) Quantification of cells containing >6 γ-H2Ax foci in siControl (n=304) and siHMGA1 (n=309) transfected cells from three independent experiments. (G, H) FISH against the rDNA intergenic spacer (IGS) (green), {AATAT}$_n$ (red) and {AAGAG}$_n$ (blue) on mitotic chromosomes from control (*nos>Omi*^{RNAi}, n=27) and *D1* mutant (*nos>Omi* ^{RNAi}; *D1*^{LL03310}/*Df*, n=57) testes co-stained for DAPI (grey). Arrowheads point to chromosome breaks.

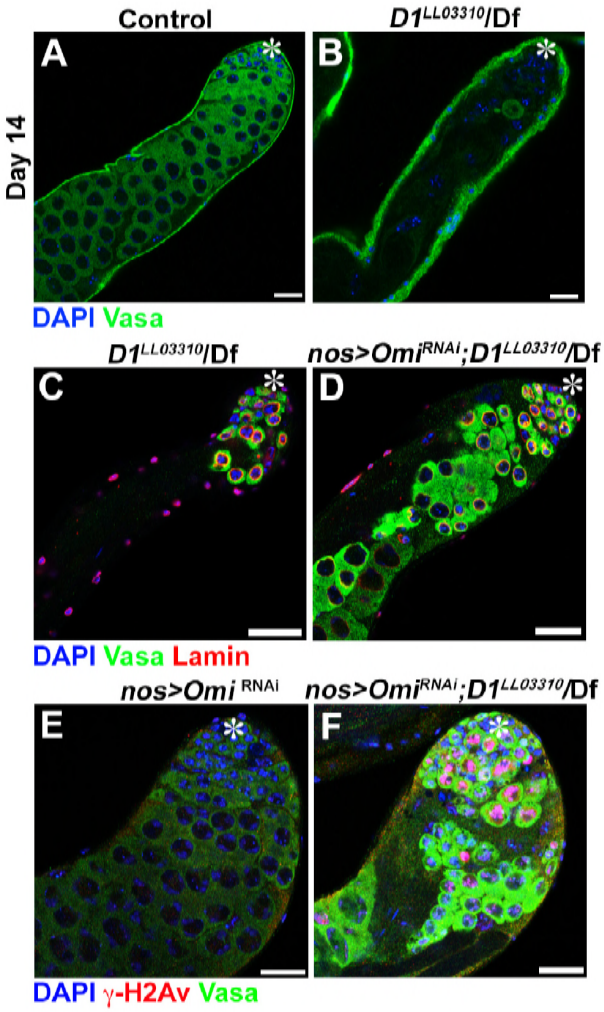

Figure 3 –figure supplement 1. Chromocenter disruption results in germ cell death in Drosophila in an Omi-dependent manner.

(A, B) Representative images of 14-day-old control ($D1^{LL03310}$/+, n=18) and $D1^{LL03310}/Df$ (n=12) testes stained for DAPI (blue) and the germ cell marker, Vasa (green). Asterisk indicates apical tip. Bars: 25μm (C, D) Representative images of *D1* mutant testes ($D1^{LL03310}/Df$) without (C) and with (D) germ cell death suppression by *Omi* knockdown ($nos>Omi^{RNAi}$), stained for DAPI (blue), Vasa (green) and $LaminDm_0$ (red) at 7 days post eclosion. (E, F) Representative images of control ($nos>Omi^{RNAi}$, $D1^{LL033010}$/+, n=10) and *D1* mutant ($nos>Omi^{RNAi}$; $D1^{LL03310}/Df$, n=13) testes stained for DAPI (blue), Vasa (green) and γ-H2Av (red).

Figure 4

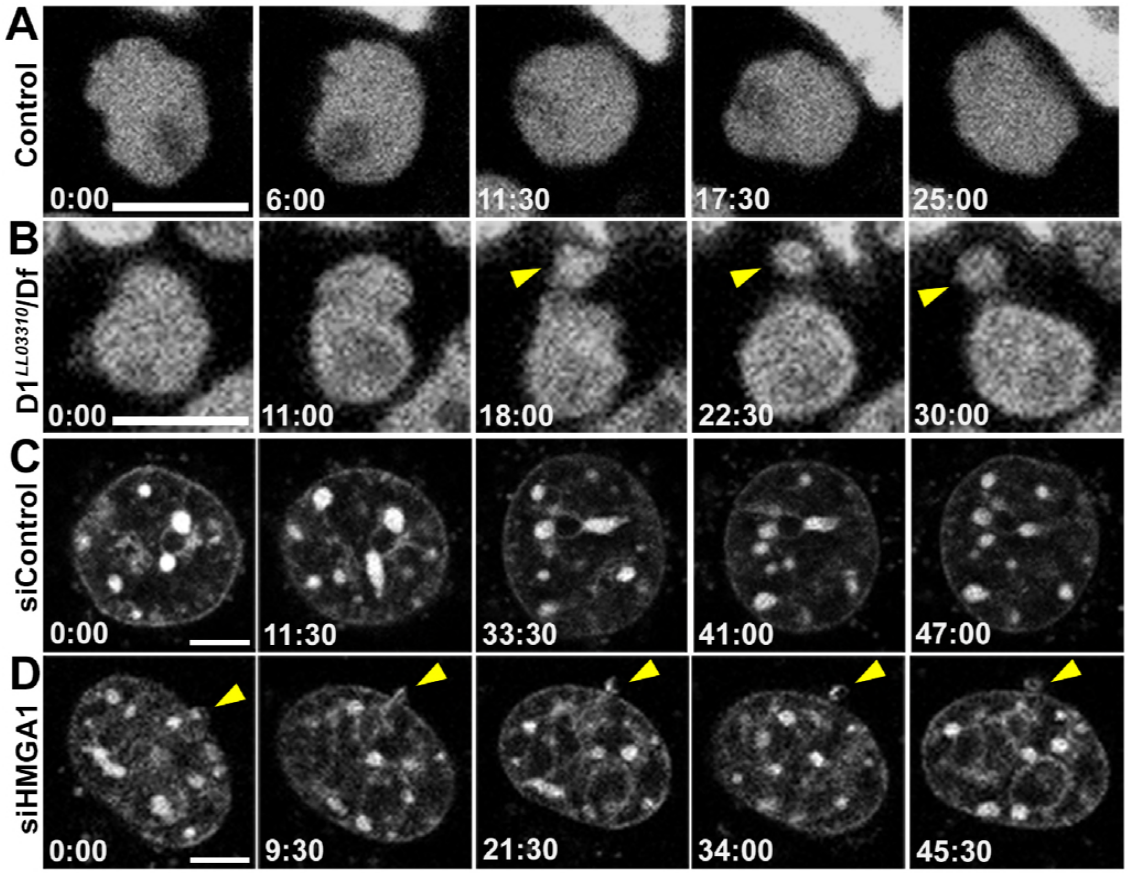

642

643 **Figure 4. D1/HMGA1 loss of function results in micronuclei formation due to nuclear**
644 **budding during interphase.**

645 (A, B) Time-lapse live imaging of control (+/+) (A) and *D1*^{LL03310}*/Df* (B) spermatogonial cells
646 expressing Df31-GFP as a nuclear marker. (C, D) Time-lapse live imaging of siControl (C) and
647 siHMGA1 (D) MOVAS cells stained with Hoechst 33342. Arrowheads indicate site of
648 micronucleus budding. Time is indicated in mm:ss. Scale bars: 5μm.

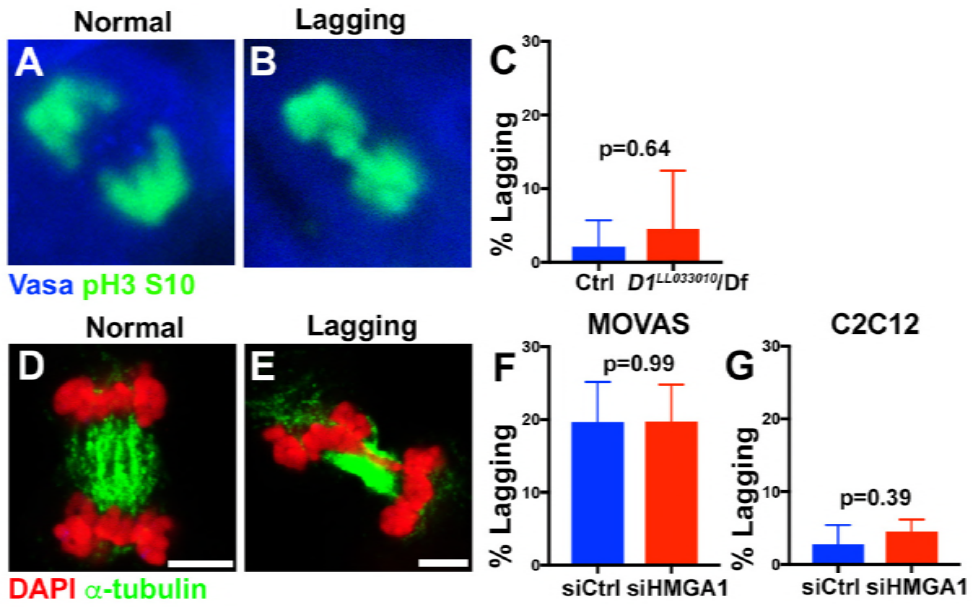

649

650 **Figure 4-figure supplement 1. Micronuclei formation upon chromocenter disruption is not**
651 **a result of mitotic lagging chromosomes.**

652 (A, B) Examples of normal and lagging mitotic chromosomes in *Drosophila* spermatogonia
653 stained for Vasa (blue) and pH3-S10 (green). (C) Quantification of spermatogonia with lagging
654 chromosomes from control ($D1^{LL033010}$/+, n=43) and $D1^{LL03310}$/*Df* (n=47) from three independent
655 experiments. P value from student's t test is shown. Error bars are SD. (D, E) Examples of
656 normal and lagging mitotic chromosomes in mouse cells stained for DAPI (red) and α-tubulin
657 (green). Bars: 5μm. (F) Quantification of mitotic cells with lagging chromosomes from siControl
658 (n=149) and siHMGA1 (n=174) transfected MOVAS cells from three independent experiments.
659 (G) Quantification of mitotic cells with lagging chromosomes from siControl (n=110) and
660 siHMGA1 (n=129) transfected C2C12 cells from three independent experiments.

661

Figure 5

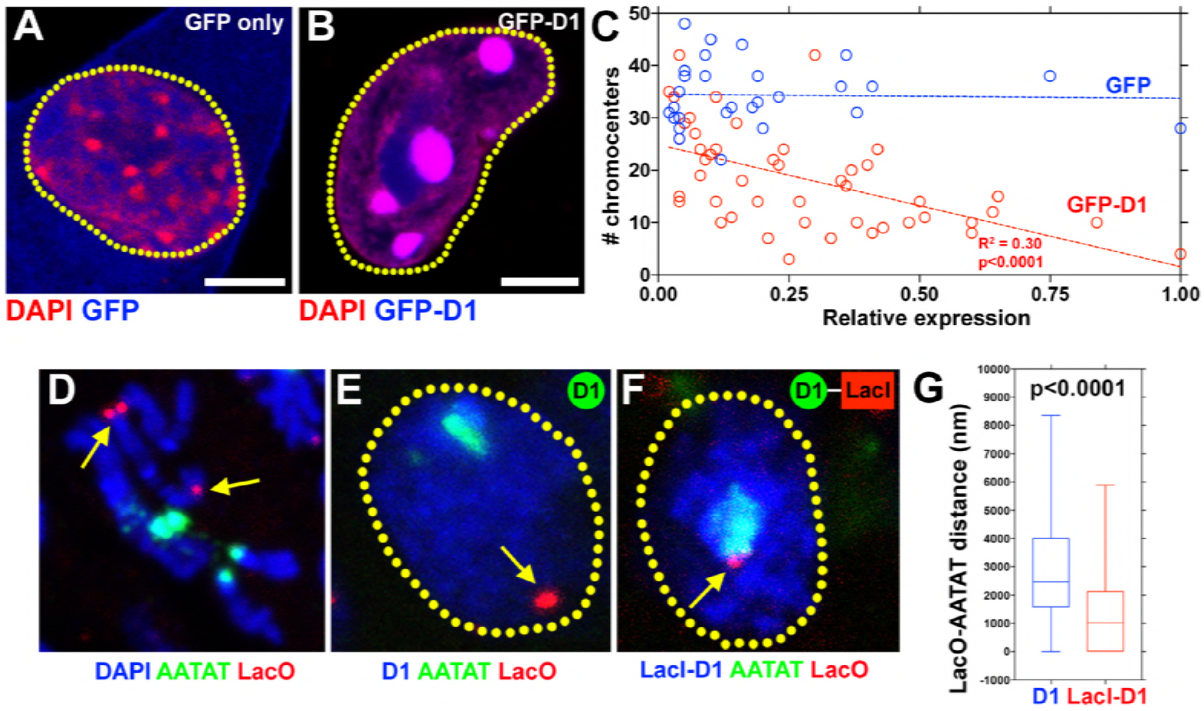

Figure 5. D1/HMGA1 bundles satellite DNA from heterologous chromosomes to form chromocenter.

(A, B) C2C12 cells expressing GFP only (blue) (A) or GFP-D1 (blue) (B) stained for DAPI (red). Dotted lines indicate nucleus. (C) Quantification of chromocenter number relative to expression level of GFP (n=29) or GFP-D1 (n=47). P value and R^2 value are indicated from linear regression analysis. (D) FISH against LacO (red) and $\{AATAT\}_n$ (green) on mitotic neuroblast chromosomes from the LacO strain stained for DAPI (blue), indicating the sites of LacO insertion (arrows). (E, F) FISH against LacO (red) and $\{AATAT\}_n$ (green) in spermatogonia expressing GFP-D1 (blue) (E) or GFP-LacI-D1 (blue) (F). Arrows indicate location of LacO sequence. (G) AATAT-LacO distance (nm) in GFP-D1 (n=97) and GFP-LacI-D1 (n=69) expressing spermatogonia. P value from student's t-test is shown. Error bars: SD. All scale bars: 5μm.

Figure 6

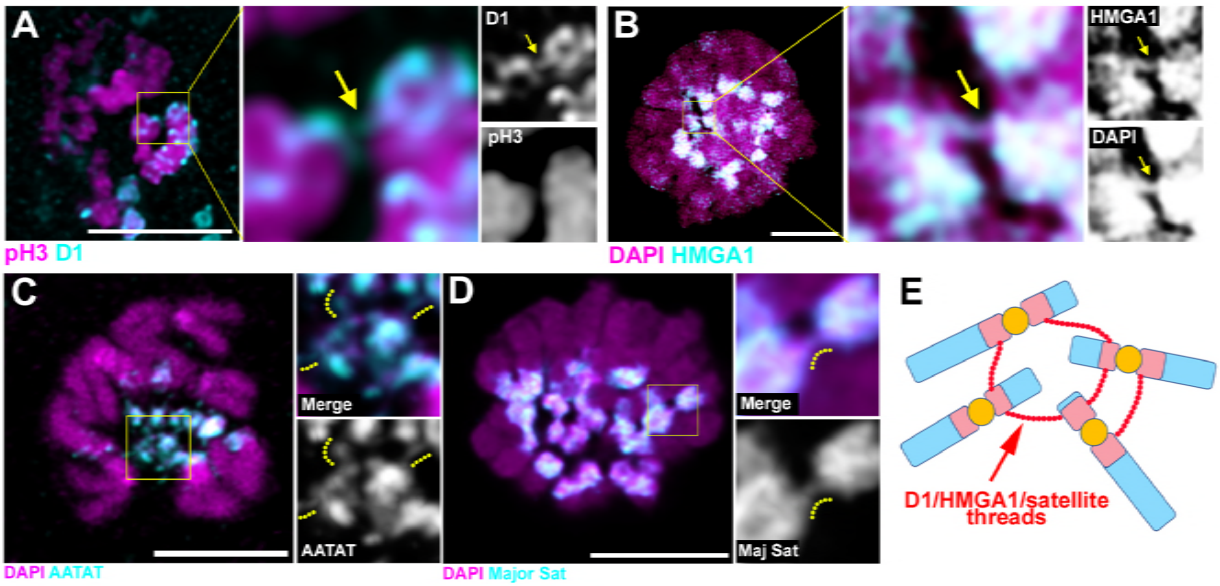

677
678 **Figure 6. D1/HMGA1 and satellite DNA form chromatin threads that link chromosomes**.
679 (A) Deconvolution microscopy performed on *Drosophila* mitotic neuroblasts stained for D1
680 (cyan) and pH3-S10 (magenta). Arrows in magnified images indicate D1-positive thread
681 connecting two chromosomes. (B) Deconvolution microscopy performed on CSK-extracted
682 RAW 264.7 macrophages stained for HMGA1 (cyan) and DAPI (magenta). Arrows in magnified
683 images indicate HMGA1-positive thread connecting two chromosomes. (C) Deconvolution
684 microscopy performed on neuroblast mitotic chromosomes stained for DAPI (magenta) and
685 FISH against $\{AATAT\}_n$ (cyan) from a *Drosophila* strain containing AATAT-rich B
686 chromosomes (Bauerly et al., 2014). Dotted lines in magnified images indicate AATAT-positive
687 threads connecting heterologous chromosomes. (D) Deconvolution microscopy performed on
688 RAW 264.7 macrophages stained for DAPI (magenta) and FISH against major satellite (cyan).
689 Dotted lines in magnified images indicate major satellite-positive threads connecting two
690 chromosomes. (E) The model of chromosome bundling by D1/HMGA1 and satellite DNA.